CFD MODELLING OF SWIRLING MECHANISM TO REDUCE EROSION OF PIPE BEND IN PNEUMATIC CONVEYING SYSTEM

Reference NO. IJME 1364, DOI: 10.5750/ijme.v1i1.1364

Bharat Singh Yadav*, Department of Mechanical Engineering, Delhi Technological University, Delhi 110042, India, **Rajiv Chaudhary and R.C. Singh**, Department of Mechanical Engineering, Delhi Technological University, Delhi 110042, India

* Corresponding author. Bharat Singh Yadav (Email): bharat_2k19phdme22@dtu.ac.in

KEY DATES: Submission date: 21.11.2023 / Final acceptance date: 26.02.24 / Published date: 12.07.2024

SUMMARY

Dry powders mixed with air transportation had bend erosion issues. CFD analysis by Shear-Stress Transport (SST) k-ɯ Model within Ansys was used to conduct a comprehensive numerical analysis of particle erosion within a 90° mild steel pipe bend in Pneumatic Conveying System. Part of the conveying pipe rotation achieved with the external motor swirling device was used to create swirling of particle before bend. Different-sized sand particles at different rpm were tested with and without a swirling device. Reduction in erosion rate of pipe bend carries significant implications, notably an extension of the system's operational lifespan. Reduction in erosion rate reports an impressive increase of 50% bend lifespan at higher RPM levels of the swirling device. The results underscore the effectiveness of this device in mitigating erosion, with significant implications for enhancing the longevity and reliability of bend life in piping systems of Pneumatic Conveying applications.

KEYWORDS

Bend, Swirling Device, Mean Effective Particle (mep) Size, Erosion Rate

NOMENCLATURE

υ	Kinematic viscosity (N s m^{-2})
ρ	Density of water (kg m^{-3})
P	Pressure (N m^{-2})
v	Velocity (m/sec)
m	Mass Flow Rate kg/sec
ϕ	Form Factor
PCS	Pneumatic Conveying System
mep	Mean Effective Particle Size of Silica, µm

1. INTRODUCTION

In the complex landscape of particle erosion, several factors play pivotal roles in determining erosion rates, as outlined in PCS [1]. These factors, including particle properties (size, hardness, velocity), fluid characteristics, and surface geometries, collectively influence the erosive behavior within oil and gas production systems. Comprehensive consideration of these factors is essential for engineering robust solutions that safeguard system integrity and minimize bend erosion-related challenges, ensuring the reliability and longevity of these critical systems."

The angle at which sand particles impact is a significant factor in surface erosion. Considerable research has been carried out in this field, leading to the creation of both theoretical and empirical erosion models.

According to Singh et al. [1], in design calculations, the flow velocity should be the most important factor to consider. The "erosional velocity" should be established based on the pipeline flow velocity, denoted as Ve [feet/sec]. This value indicates the velocity threshold at which erosion is likely to occur, serving as a marker for the velocity level where erosion could potentially take place.

$$v_e = \frac{c}{\sqrt{\rho}} \tag{1}$$

The variable C is an empirical constant, while ρ signifies the density of the fluid combination, measured in [lbs/ft^3].

Nonetheless, according to Salama et al. [12], erosion typically occurs only at very high velocities in solids-free fluids.

These guidelines are based on the work of Salama et al. [12], and they provide insights into selecting the appropriate value of C for different scenarios. The constant C is crucial for calculating particle erosion in pipe bends, as outlined in Ababaei et al. [2].

According to Durate et al. [3], the preferred approach for complex piping layouts or scenarios where erosion location is of utmost significance is to perform Computational Fluid Dynamics (CFD) erosion simulations.

1.1 BACKGROUND

Pneumatic conveying serves as a widely adopted method for efficiently transporting dry powders and granular particles through pipelines and bends using high-pressure gas or air. This approach finds extensive use for short-distance material transfer within various industries and plants. Its appeal lies in the flexibility it offers for routing pipelines and its capacity to reduce dust levels.

1.2 WEAR IN PIPE BEND

Within pneumatic conveying pipelines, particles are afforded the liberty to roll, slide, and make contact, thus introducing intricate material removal processes on the surfaces of pipe bends. This phenomenon is commonly termed as the wear of the bend's wall material. This wear can intensify, eventually leading to the development of punctures in the pipe bend, as depicted in Figure 1. It's worth noting that the majority of material loss typically accumulates in the vicinity of these punctured areas. Therefore, it becomes paramount to attain a comprehensive understanding of the wear mechanisms around pipe bend punctures. This comprehension can be crucial in diminishing the occurrence of failures and prolonging the overall operational lifespan of pneumatic conveying pipelines.

2. CFD SIMULATION

The essence of CFD lies in its ability to translate the complexities of fluid behaviour into a computationally tractable framework. By discretizing the fluid domain and applying numerical methods, CFD enables the investigation of intricate flow phenomena that might be challenging or even impossible to analyze experimentally. This capability has made CFD a cornerstone in addressing diverse challenges, from optimizing aerodynamic profiles for aircraft and automobiles to enhancing the efficiency of heat exchangers and understanding biological fluid dynamics.

Moreover, CFD provides the advantage of gaining insights into fluid dynamics under a wide range of conditions, from the macroscopic world of industrial processes to the microscopic realm of biofluids and environmental systems. It allows for the exploration of transient and turbulent flows, laminar regimes, and multiphase interactions. As computational resources and simulation techniques continue to advance, CFD remains at the forefront of research and development, contributing to innovations and advancements in various scientific and engineering fields.

2.1 CAD MODEL SETUP

At the beginning of the study, design a CAD model of a bend with the help of CATIA software. For case 1, a simple bend was designed without a swirling device shown in Fig. 2. But in other cases, a swirling device was used for the study; the light blue colour is the bend pipe, and the yellow colour shows the swirling device's location in Fig. 3 The design dimensions of the bend pipe and swirling device are given in Table 1.

2.2 MESHING

In ANSYS CFD modelling, nodes and elements are created to occupy the entire flow volume, forming a mesh. Each cell within this mesh represents a distinct region that characterizes the local flow. Mathematical equations, which govern the flow physics, are subsequently applied to each cell in the mesh. The quality of this mesh is of utmost importance as it directly impacts the reliability of the solutions obtained and ensures numerical stability. In the current study, the CAD model of the pipe bend was divided into 13,320 nodes and 11,456 elements.

2.3 CFD SIMULATION MODEL

- First define the Steady Flow Model for the study of two bend Designs in the XZ H-plane with gravity in the Y direction is 9.81m/s2.
- The working fluid is the main important factor in CFD in this study air as the working fluid for the study.
- The defined temperature is 27^{o}C, the specified air density is 1.293kg/m^3, and the specified viscosity is 1.810-5 kg.m^{-1}. s^{-1}. Choosing inlet type as velocity inlet and inlet velocity on the system was U = 23.11 m/s.
- In our study, we simulate turbulence using a standard k-two equations turbulence model. This model is constructed using transport equations for both turbulence kinetic energy (k) and dissipation rate (ε). It's important to note that this model applies only to fully turbulent flows. To depict wall-bounded turbulent flows, we utilize scalable wall functions. Notably, our turbulence model has undergone revisions to allow for the resolution of the viscosity-affected region, encompassing the viscous sublayer, through a mesh that extends to the wall. This approach enhances the accuracy of our simulations near the boundary surfaces. CFD boundary conditions are shown in Table 1 and material properties are shown in Table 2.

2.4 CFD GOVERNING EQUATIONS

These are Reynold's equations which govern the CFD in the Ansys program. The various governing equations are given below.

2.4.1 Viscous -SST K-omega

The SSk-turbulence model, first developed by Menter in 1993, stands as a prominent example of a two-equation eddy-viscosity model. In the field of turbulence modelling, the pursuit of a versatile approach has led to the creation

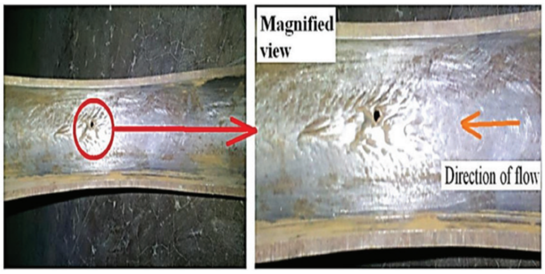

Figure 1. Photograph depicting a punctured pipe bend

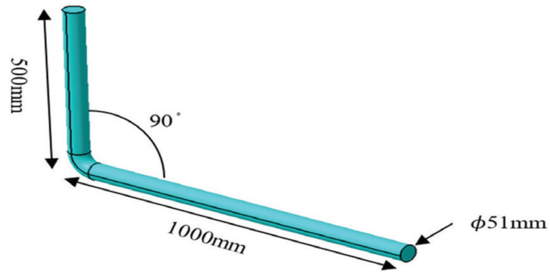

Figure 2. Simple L bend

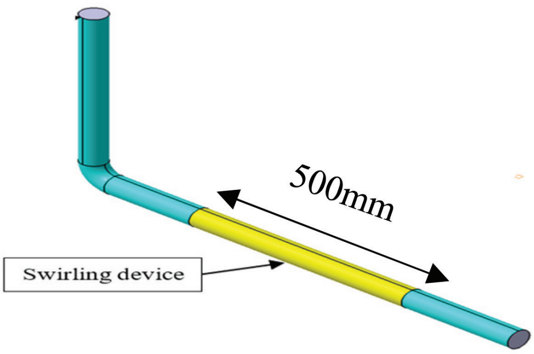

Figure 3. Bend with swirling device

Table 1. Model dimensions

Model Parameters	**Dimensions**
Horizontal Length (mm)	1000
Vertical Length (mm)	500
Swirling device length (mm)	500
Diameter of Pipe (mm)	51
Angle (°)	90

of the shear stress transport (SST) model, which combines various advantages effectively. The k-model within the SST serves as a robust Low-Re turbulence model, eliminating the need for additional damping functions by incorporating a k- formulation within the inner regions of the boundary layer. What sets this model apart is its unique ability to extend its applicability to the wall, encompassing even the viscous sub-layer. This distinguishes it from conventional k-models, known for their sensitivity to free-stream turbulence conditions at the inlet.

Table 2. CFD boundary condition

Boundary Condition		
Rotary feeder speed (RPM)	125	
Pressure of root blower (Bar)	1	
Free air CFM (m^3/sec)	100CFM=0.0472	
Cycle time (sec.)	45*60=2700	
Mass flow rate (Particle) (kg/Sec)	0.074	
Mass flow rate (Air) (kg/Sec)	0.0547	
Inlet velocity (Air) (m/sec)	23.11	
Swirling device speed (rpm)	35,70,100	
Distance of swirling device from bend (m)	0.5	
CFD Material Properties		
	Silica	**Air**
Density (kg/m^3)	2000	1.293
Viscosity (kg. $m^{-1}.s^{-1}$)	-	1.8×10^{-5}
Particle size (µm)	200,250,300	-

2.4.2 Kinematic Eddy Viscosity

$$\nu_T = \frac{a_1 k}{\max\left(a_1\omega,\ SF_2\right)}$$

2.4.3 Turbulence Kinetic Energy

$$\frac{\partial k}{\partial t} + U_j\frac{\partial k}{\partial x_j} = P_k - \beta^* k\omega + \frac{\partial}{\partial x_j}\left[\left(\nu + \sigma_k \nu_T\right)\frac{\partial k}{\partial x_j}\right] \quad (1)$$

2.4.4 Specific Dissipation Rate

$$\frac{\partial \omega}{\partial t} + U_j\frac{\partial \omega}{\partial x_j} = \alpha S^2 - \beta\omega^2 + \frac{\partial}{\partial x_j}\left[\left(\nu + \sigma_\omega \nu_T\right)\frac{\partial \omega}{\partial x_j}\right] + 2\left(1 - F_1\right)\sigma_{\omega 2}\frac{1}{\omega}\frac{\partial k}{\partial x_i}\frac{\partial \omega}{\partial x_i} \quad (2)$$

2.4.5 Closure Coefficients and Auxiliary Relations

$$F_2 = \tanh\left[\max\left(\frac{2\sqrt{k}}{\beta^*\omega y}, \frac{500\nu}{y^2\omega}\right)\right]^2$$

$$P_k = \min\left(\tau_{ij}\frac{\partial U_i}{\partial x_j}, 10\beta^* k\omega\right)$$

$$F_1 = \tanh\left\{\left\{\min\left[\max\left(\frac{\sqrt{k}}{\beta^*\omega y}, \frac{500\nu}{y^2\omega}\right), \frac{4\sigma_{\omega 2}k}{CD_{k\omega}y^2}\right]\right\}^4\right\}$$

Table 3. CFD results

Particle Size		Unit	Bend (without swirling device)	Bend-1 (Swirling device with 35rpm)	Bend-2 (Swirling device with 70 rpm)	Bend-2 (Swirling device with 100 rpm)
200	Erosion rate	mm/year	8.0	6.42	5.14	4.0
	Velocity	m/s	31.3	40.6	52.8	68.7
250	Erosion rate	mm/year	10.0	8.03	6.42	5.0
	Velocity	m/s	37.5	48.8	63.4	82.4
300	Erosion rate	mm/year	12.0	9.63	7.70	6.0
	Velocity	m/s	53.0	68.9	89.6	116.4

$$CD_{k\omega} = \max(2\rho\sigma_{\omega 2}\frac{1}{\omega}\frac{\partial k}{\partial x_j}\frac{\partial \omega}{\partial x_i}, 10^{-10}) \quad (3)$$

$$\phi = \phi_1 F_1 + \phi_2 (1 - F_1)$$

$$\alpha_1 = \frac{5}{9}, \alpha_2 = 0.44$$

$$\beta_1 = \frac{3}{40}, \beta_2 = 0.0828$$

$$\beta^* = \frac{9}{100}$$

$$\sigma_{k1} = 0.85, \sigma_{k2} = 1$$

$$\sigma_{\omega 1} = 0.5, \sigma_{\omega 2} = 0.856$$

2.5 DISCRETE PHASE MODELLING

Sand is the discrete phase, with specific properties such as a density of 2500 kg/m³, a flow rate of 0.1 kg/s, and a particle diameter of 1000 µm. To accommodate the non-spherical shape of these sand particles, we employ a non-spherical drag law, as described in the same reference [7].

where: C_D represents the drag coefficient and Re_D the

$$C_D = \frac{24}{\mathrm{Re}_D}\cdot\left(1 + b_1 \cdot \mathrm{Re}_D^{b_2}\right) + \frac{b_3 \cdot \mathrm{Re}_D}{b_4 + \mathrm{Re}_D} \quad (4)$$

Reynolds number.
The values for the b1, b2, b3 and b4 coefficients are calculated as follows:

$$b_1 = \exp\left(2.3288 - 6.4581\phi + 2.4486\phi^2\right) \quad (5)$$

$$b_2 = 0.0964 + 0.5565\phi \quad (6)$$

$$b_3 = \exp\left(4.905 - 13.8944\phi + 18.4222\phi^2 - 10.2599\phi^3\right) \quad (7)$$

$$b_4 = \exp\left(1.4681 + 12.2584\phi - 20.7322\phi^2 + 15.8855\phi^3\right) \quad (8)$$

Where ϕ stands for the form factor,

$$\phi = \frac{s}{S} \quad (9)$$

S is the actual surface area of the particle, while s is the surface area of a sphere with the same volume as the particle. For the CFD analysis, a sand particle form factor of = 0.9 was chosen.

3. RESULTS AND DISCUSSIONS

As per Computational fluid dynamic results, the maximum erosion rates in mm/year for pipe bends with density ρ = 7850 Kg/m³ are shown in Table 3.

Case-1 Particle size 200 and without a swirling device.

In case-1 particle size was 200µm. The velocity in this case increases up to 31.3m/s pipe total erosion rate is 8.0mm/year. The CFD results contours are shown in Fig.4.

Case-2 Particle size 250 and without swirling device.

In case-2 particle size was 250µm. The velocity in this case increases up to 37.5m/s pipe total erosion rate is 10.0mm/year. The CFD results contours are shown in Fig. 5.

Case-3 Particle size 300 and without swirling device.

In case-3 particle size was 300µm. The velocity in this case increases up to 53.0m/s pipe total erosion rate is 12.0mm/year.

Case-4 Particle size 200 and with swirling device 35rpm

In case-4 particle size was 200 µm. The velocity in this case increases up to 40.6m/s pipe total erosion rate is 6.42mm/year. The CFD results contours are shown in Fig. 6.

Case-5 Particle size 250 and with swirling device 35rpm

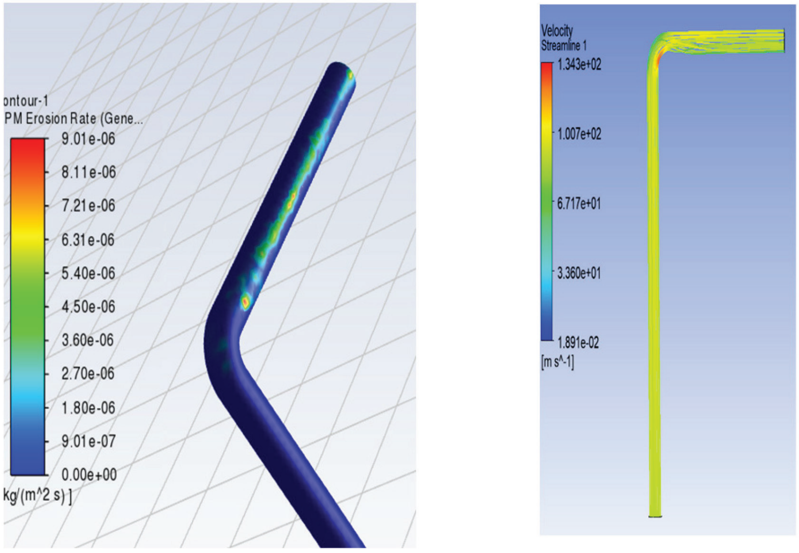

Figure 4. Erosion rate and velocity at 200 µm particle size without swirling device

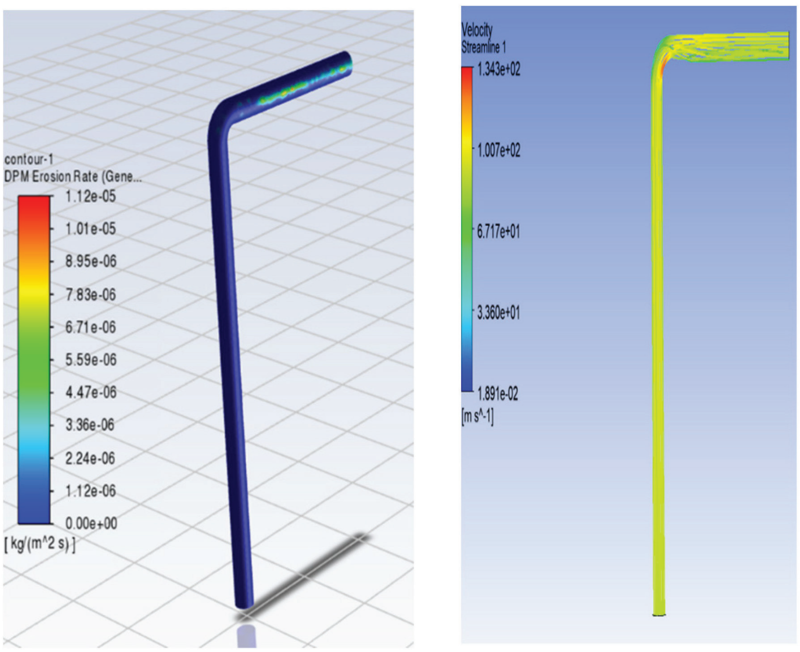

Figure 5. Erosion rate and velocity at 250 µm particle size without swirling device

In case-5 particle size was 250 µm. The velocity in this case increases up to 48.3m/s pipe total erosion rate is 8.03mm/year. The CFD results contours are shown in Fig.7

Case-6 Particle size 300 and with swirling device 35rpm

In case-6 particle size was 300 µm. The velocity in this case increases up to 68.9m/s pipe total erosion rate is 9.63mm/year. The CFD results contours are shown in Fig.8

Case-7 Particle size 200 and with swirling device 70rpm

In case-7 particle size was 200 µm. The velocity in this case increases up to 52.8m/s pipe total erosion rate is 5.14mm/year.

Case-8 Particle size 250 and with swirling device 70rpm

In case-8 particle size was 250 µm. The velocity in this case increases up to 63.4m/s pipe total erosion rate is 6.42mm/year.

Case-9 Particle size 300 and with swirling device 70rpm

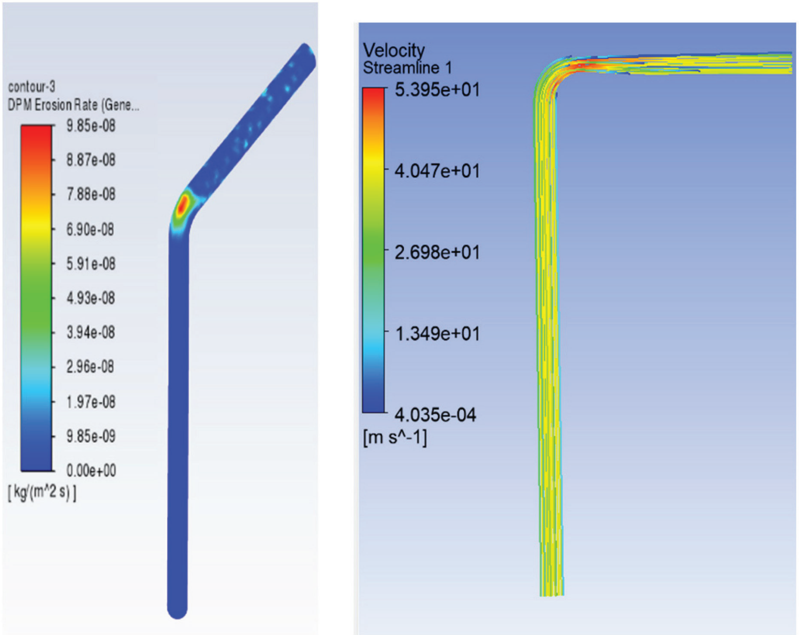

Figure 6. Erosion rate plot and velocity plot at 200 µm particle size with swirling device (35rpm)

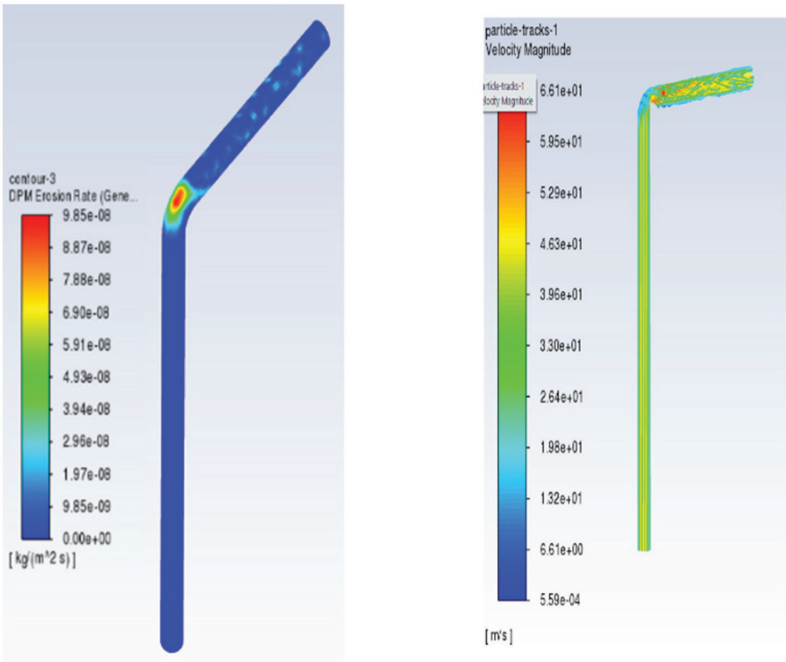

Figure 7. Erosion rate plot and velocity plot at 250 µm particle size with swirling device (35rpm)

In case-9 particle size was 300 µm. The velocity in this case increases up to 89.6m/s pipe total erosion rate is 7.70mm/year.

Case-10 Particle size 200 and with swirling device 100rpm

In case-10 particle size was 200 µm. The velocity in this case increases up to 68.7m/s pipe total erosion rate is 4.0mm/year.

Case-11 Particle size 250 and with swirling device 100rpm

In case-11 particle size was 250 µm. The velocity in this case increases up to 82.4m/s pipe total erosion rate is 5.0mm/year.

Case-12 Particle size 300 and with swirling device 100rpm

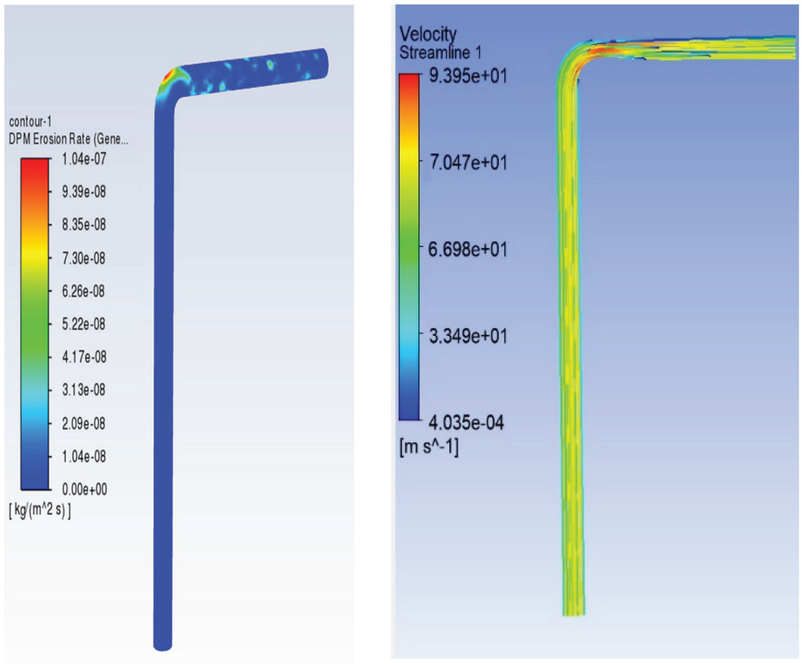

Figure 8. Erosion rate plot and velocity plot at 300 µm particle size with swirling device (35rpm)

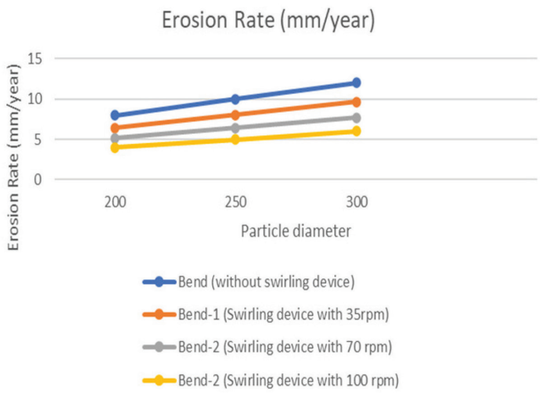

Graph 1. Erosion rate graph at different bend conditions

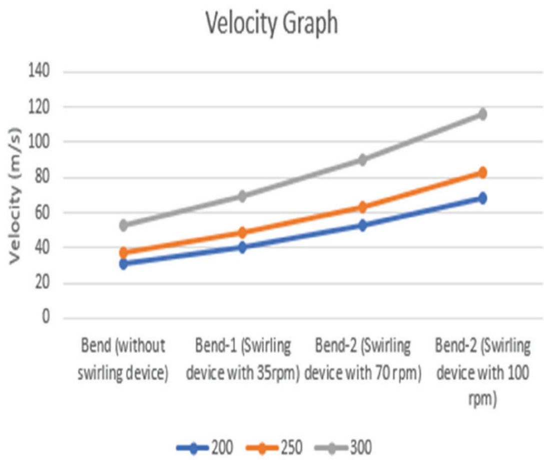

Graph 2. Velocity graph at different bend conditions

In case-30 particle size was 300 µm. The velocity in this case increases up to 116.4m/s pipe total erosion rate is 5.0mm/year.

Erosion rate Graph 1: The erosion rate increases with increasing the diameter of sand particles. The given graph shows the erosion rate at different particle diameters. In this study, case-10 shows the Minimum erosion rate and case-3 maximum erosion rate. In the given study swirling device was not used in case-3. Due to this maximum erosion occurs. In case 10 swirling device with 100 rpm was used for the study. so due to the swirling devise erosion rate in case-10 decreased due to the swirling effect.

Velocity Graph 2: The velocity increases with increasing the rpm of the swirling device. The given graph shows the velocity at different RPMs in this study case-10 shows the maximum velocity rate and case-3 minimum velocity.

In the given study swirling device was not used in case-3. Due to this minimum velocity occurs. In case 10 swirling device with 100 rpm was used for the study so due to swirling devise velocity in case-10 increases due to the swirling effect.

4. CONCLUSIONS

In this study, an erosion model based on Computational Fluid Dynamics (CFD) is employed to assess the erosion rate under different conditions, including various particle sizes and RPMs (Revolutions Per Minute). Additionally, the study delves into the calculation of particle velocity and the investigation of particle size as part of the analysis. Based on the data of Table 3, the following conclusion can be reached:

- Figure 6 depicts the maximum erosion rates for a 90° bend without a swirling device.
- The higher erosion rate causes system failure and reduces the life cycle of the system.
- In the case of a 90º bend with a swirling device, it's observed that the maximum erosion rate decreases as the swirling device's RPM (Revolutions Per Minute) increases. This decrease in erosion rate is directly associated with an increase in the system's operational lifespan.
- In the absence of a swirling mechanism, when a particle strikes the L-tube wall, silica particles swirl. The highest velocity increase among the particles reaching the bend intrados is predicted to occur at the 90º bend.
- Then in this study swirling device is used for decrease erosion rate. The swirling device swirl sand particle before hitting the pipe and reduce erosion rate.
- In the current analysis the erosion rate in bend pipe decreases up to 6.0mm/year at higher RPM and the overall life of the system increases 50% at higher RPM.

5. ACKNOWLEDGMENT

The faculty and supporting staff of design center and CAD Centre Mechanical Engg, Department of DTU are acknowledged for providing Ansys Software workstation.

6. REFERENCES

1. SINGH, J., KUMAR, S., SINGH, J. P., KUMAR, P., and MOHAPATRA, S. K. (2019). *CFD modeling of erosion wear in pipe bend for the flow of bottom ash suspension*. *Particulate Science and Technology*, *37*(3), 275-285.
2. ABABAEI, A., ABBASIAN ARANI, A. A., and AGHAEI, A. (2017). *Numerical investigation of forced convection of nanofluid flow in microchannels: effect of adding micromixer*. *Journal of Applied Fluid Mechanics*, *10*(6), 1759-1772.
3. DUARTE, C. A. R. and DESOUZA, F. J. (2017). *Innovative pipe wall design to mitigate elbow erosion: A CFD analysis*. *Wear*, *380*, 176-190.
4. SHYJI, S., DEEPU, M., KUMAR, N. A. and JAYACHANDRAN, T. (2017). *Numerical studies on thrust augmentation in high area ratio rocket nozzles by Secondary injection. Journal of Applied Fluid Mechanics*, *10*(6), 1605-1614.
5. SINGH, J. P., KUMAR, S. and MOHAPATRA, S. K. (2017). *Modelling of two phase solid-liquid flow in horizontal pipe using computational fluid dynamics technique. International journal of hydrogen energy*, *42*(31), 20133-20137.
6. SADRIZADEH, S., NEJAD GHAFAR, A., HALILOVIC, A. and HÅKANSSON, U. (2017). *Numerical, experimental and analytical studies on fluid flow through a Marsh funnel. Journal of Applied Fluid Mechanics*, *10*(6), 1501-1507.
7. CHEN, J., WANG, Y., LI, X., HE, R., HAN, S., and CHEN, Y. (2015). *Erosion prediction of liquid-particle two-phase flow in pipeline elbows via CFD–DEM coupling method. Powder Technology*, *275*, 182-187.
8. CHEN, L., DUAN, Y., PU, W. and ZHAO, C. (2009). *CFD simulation of coal-water slurry flowing in horizontal pipelines*. Korean journal of chemical engineering, 26, 1144-1154.
9. CHEN, X., MCLAURY, B. S. and SHIRAZI, S. A. (2004). *Application and experimental validation of a computational fluid dynamics (CFD)-based erosion prediction model in elbows and plugged tees. Computers & Fluids*, *33*(10), 1251-1272.
10. BARTON, N. A. (2003). *Erosion in elbows in hydrocarbon production systems*: Review document.
11. DNV, G. (2015). *Recommended Practice–DNVGL-RP-O501–Managing Sand Production and Erosion. DNV GL: Akershus, Norway*, 3-60.
12. VENKATESH, E. S. (1986, May). *Erosion damage in oil and gas wells. In SPE Rocky Mountain* Petroleum Technology Conference/ Low-Permeability Reservoirs Symposium (pp. SPE-15183). SPE.
13. PETERS J (2014). *NEL UK Erosion Management Using Erosion Testing Combined with Erosion* 6th European Sand Management Forum Aberdeen 26-27.
14. FINNIE I and MCFADDEN D (1978). *On the velocity dependence of the erosion of ductile metals by solid particles at low angles of incidence* Wear 48(1), 181-190.
15. NEILSON J and GILCHRIST A (1968). *Erosion by a stream of solid particles* Wear 11(2), 111-122.
16. MCLAURY B S (1996). Predicting Solid Particle Erosion Resulting from Turbulent Fluctuations in Oilfield Geometries University of Tulsa PhD Thesis.
17. AHLERT K R (1994). Effects of particle impingement angle and surface wetting on solid particle erosion of AISI 1018 Steel University of Tulsa MSc Thesis.
18. SALAMA M M and VENKATESH E S (1983). Evaluation of Erosional Velocity Limitations in Offshore Gas Wells 15th Annual Offshore Technology Conference Houston Texas May 2 – 5, 371– 376.
19. OKA Y I, OKAMURA K and YOSHIDA T (2005) Practical estimation of erosion damage caused by solid particle impact: Part 1: Effects of impact parameters on a predictive equation Wear 259(1)pp 95-101.

20. EDWARDS, J. K., MCLAURY, B. S., and SHIRAZI, S. A. (2000). *Evaluation of Alternative Pipe Bend Fittings in Erosive Service,"Paper* No. In *FEDSM00-11245, ASME Fluids Engineering Division Meeting, Boston, MA*.
21. MOHYALDIN M. E., ELKHATIB N. and ISMAIL M. C. (2011). *Evaluation of different modelling methods used for erosion prediction in Proceedings of the NACE Corrosion* Shanghai Conference & Expo. 2011, 1-19.
22. BOURGOYNE, A. T. (1989). *Experimental Study of Erosion in Diverter Systems Due to Sand Production.* Society of Petroleum Engineers. doi:10.2118/18716-MS.